ISSN: 0067-2904

Study Effects of Illumination and Temperature on Performance of (pn-Si) Device using Simulation Program SCAPS-1D

Raad A.Rassol*, Ali A Mohammed, Rasha F.Hasan
University of Mosul , Education College of Pure Science ,Physics Department

Received: 9/7/2020 Accepted: 30/8/2020

Abstract

The current research included obtaining the best performance specifications for a silicon device with a mono-crystalline type pn junction (pn–Si). A simulation of the device was performed by the use of a computer program in one dimension SCAPS-1D in order to reach the optimum thickness for both p and n layers and to obtain the best efficiency in performance of the pn-Si junction. The optimum device efficiency was eta (η) = 12.4236 % when the ideal thickness for the p and n layers was 5µm and 1.175µm, respectively (p=5 µm and n=1.75µm).

The research included studying the effects of different spectra of solar illumination using simulation of the device; the usual solar spectrum AM1_5 G1 sun. Spectrum, Black body spectrum, White spectrum constant photon flux, White spectrum constant photon power, Monochromatic spectrum constant flux, and Monochromatic spectrum constant power. The highest efficiency was obtained from the monochrome spectrum with constant power (eta (η) =22.4338 %). The effects of different temperatures on the device was studied on 250K, 300K, 350K, 400K, and 450K. The highest efficiency was revealed for Monochromatic spectrum constant power (eta (η) =24.5381 %) when the temperature was 250K.

Key Words: Thin Film Solar-Cells, (pn-Si) Junction, solar spectrum, program computer SCAPS−1D.

دراسة تأثير الإضاءة ودرجة الحرارة على أداء النبيطة (pn–Si) باستخدام برنامج المحاكاة SCAPS–1D

رعد أحمد رسول*، علي عباس محمد، رشا فيصل حسن
جامعة الموصل، كلية التربية للعلوم الصرفة، قسم الفيزياء

الخلاصة

يتضمن البحث الحصول على أفضل مواصفات لأداء نبيطة مصنوعة من السليكون ذات مفرق pn من النوع أحادي التبلور(pn–Si). إذ تم إجراء محاكاة للنبيطة باستخدام البرنامج الحاسوبي في بعد واحد SCAPS–1D في التوصل إلى السُمك الأمثل لكل من طبقة p وn وللحصول على أفضل كفاءة لأداء النبيطة (pn–Si). إذ كانت كفاءة النبيطة المثلى (% 12.4236= (η) eta) عندما كان السُمك المثالي لطبقتي p و n هو 5µm و1.175µm على التوالي (p=5µm و n=1.175µm).

تضمن البحث دراسة تأثير الإضاءة الشمسية بأطيافها المختلفة ايضا باستخدام محاكاة النبيطة (الطيف الشمسي الاعتيادي AM1_5 G1، طيف الجسم الأسود، طيف الضوء الأبيض ذو الفيض الفوتوني الثابت، طيف الضوء الأبيض ذو القدرة الفوتونية الثابتة، طيف أحادي اللون ذو الفيض الثابت، وطيف أحادي اللون

*Email: dr.raadrasool@yahoo.com

ذو القدرة الثابتة). إذ تم الحصول على أعلى كفاءة من الطيف الشمسي أحادي اللون ذو القدرة الثابتة (eta
(η) =22.4338 %). تم دراسة تأثير درجات الحرارة مختلفة على النبيطة (250 K، 300 K، 350 K،
400 K 450 K). وقد تبين ان أعلى كفاءة كانت للطيف الشمسي أحادي اللون ذو القدرة الثابتة (eta (η)
=24.5381 % عند درجة الحرارة 250 K.

Introduction

The primary structure and the processes of manufacturing of dual device, including light-emitting diodes are similar to those of the solar cells manufactured on a semi-conductive silicon floor. Adding atoms of an impure doped material to silicon with a small concentration can modify the electrical properties of the crystal, allowing the formation of the p-n junction. The material doped with the donor material is called the n-type material, if it has valence electrons more than the four electrons that silicon possesses in its outer orbit; such as a phosphorus (P) atom that has five valence electrons, making covalent bonds with the four adjacent silicon atoms while the fifth electron becomes a conducting electron, as it doped to the conduction band; then silicon become of an n-type [1].

The doped material is known as accepter if the number of valence electrons is less than that in the outer orbit, as compared to silicon, since when replacing a silicon atom with a three-valence Boron atom (B) it can accept an additional electron to form four covalent bonds with silicon atoms. As a result, it generates a positive charge hole (in the valence band), where the semiconductor in this case is called *P*-type. The p-n junction consists of contacting the n-type semiconductor with the p-type semiconductor, which represents the basic structure of each two devices and solar cells. Many articles and books have been published on the physics of the junction p-n [1-3], hence only the basic model is used here to describe the response of current - voltages in solar cells. When the p-n junction is lighted, the current can flow through it, and the junction can act as a solar cell [4].

Current arises from the internal electric field generated at the silicon interface for both the n-type and p-type. Diffusion current arises from the variance in the charge carrier concentrations in the n-type and p-type region. Electrons tend to diffuse from a highly concentrated region of n-type silicon towards a lower concentration region of p-type silicon. The spread of the holes is in the opposite direction, i.e. from the high concentration region of the holes in the p-type semiconductor to the lower concentration region of the holes in the semiconductor n-type [1].

The drift current is greater than the diffusion current when the solar cell is illuminated, therefore, it creates an opposite current in the direction of the current that flows in the standard diode. According to the band theory model, the absorbed photons excite more charge carriers to the conduction band, which in turn are affected by the electric field, which causes them to drift faster. When the cell is not lighted, the current does not flow through it, as a result of the balance of the drift current and the diffusion current with each other, which flow in opposite directions [5].

In this study, the simulation program SCAPS-1D (Solar Cell Capacitance Simulator) was used to perform electrical and optical properties of solar cells with a p-n junction in one dimension using numerical simulations [6]. This program helps to simulate and analyze curves of the properties of current-voltage (I–V) and to analyze AC properties for current-frequency (I-F) and frequency-capacitance (C-F).

Each of these measurements can be calculated under conditions of light and dark and it is a function of temperature [7]. The spectral response of the Quantum Energy (QE), Fill Factor (FF), short-circuit current (Jsc), open circuit voltage (Voc), energy beams of materials used in solar cells, and the concentrations of different materials, can also be analyzed by solving basic semiconductor equations. Therefore, continuity equation and the Poisson's equation are both applied for electrons and hole [8,9].

Theoretical simulation of the solar cell and the main factors affecting it

In this study, the simulation program SCAPS-1D (Version 3307) was used to solve equations in one-dimension using basic semiconductor equations to simulate solar cells. The main equation is that of Poisson's, which connects the charge with electrostatic voltage φ and is given by the following relationship [9, 10]:

$$\frac{\partial^2 \varphi}{\partial x^2} = \frac{\rho}{\varepsilon_s} = -\frac{q}{\varepsilon_s}\left(p - n + N_d^+ + N_a^-\right) \quad \ldots\ldots\ldots (1)$$

where ε_s is the semiconductor permittivity, ρ is the charge density, q is the electric charge, n and p are the concentrations of both electrons and holes, respectively, and N_d^+ and N_a^- are the concentrations of

both donors and accepters, respectively. The continuity equation for both electrons and holes is given by the following relationship [11]:

$$J_n = -qD_n \frac{\partial n}{\partial x} + \mu_n qn \frac{\partial \varphi}{\partial x} \quad \ldots\ldots\ldots\ldots (2)$$

$$J_p = -qD_p \frac{\partial p}{\partial x} + \mu_p qp \frac{\partial \varphi}{\partial x} \quad \ldots\ldots\ldots\ldots (3)$$

where J_n and J_p represent the current density of the electrons and holes, $D_{n,p}$ are the diffusion coefficients for electrons and holes, and $\mu_{n,p}$ are the motilities of electrons and holes, respectively. The solar cell of length L can be divided into N of time periods. Values are formed of the electrostatic voltage φ_i and the concentrations of electrons and holes the n_i and J_p form each of these periods the unknowns which can be found numerically by solving 3N of nonlinear equations, because the continuity equation contains the recombination term, which is nonlinear for both electrons and holes; that is, the basic equations for each of the periods i. φ_i, E_{Fni} and E_{Fpi} can be chosen as independent variables instead of φ_i, n_i, p_i, E_{Fni} and E_{Fpi}, which represent Quasi-Fermi energy levels for both electrons and holes. The most important factors that affect the properties of solar cells are [10]:

1- Short circuit current density I_{sc}: it represents the current density that flows through the junction when it is lighted, and there is no applied bias (i.e. the applied bias is zero), while the I_{sc} short circuit current density is in an ideal case that is equal to the photo that generated the current density. Thus, the short circuit current is the highest current that flows through the solar cell when the load resistance is zero, meaning that the solar cell conducts in a short circuit.

2- Open circuit voltage V_{oc}: it represents the maximum voltage that can be obtained from the solar cell when the current that is passing through the solar cell junction is zero and the solar cell is an open circuit (i.e. the load resistance is infinite). The open circuit voltage can be expressed by the following equation:

$$V_{oc} = \frac{nkT}{q} \ln\left(\frac{I_L}{I_o} + 1\right) \quad \ldots\ldots\ldots\ldots (4)$$

where I_L represents the current generated by the incident light at p-n junction, I_o is the saturation current in the absence of light, *n* is the ideal factor, *k* is Boltzmann constant, and T is the absolute temperature. It can be noted from eq.(4) that the open circuit voltage depends on the current generated by the incident light and that the saturation current depends on the processes of recombination in the solar cell. Therefore, the open circuit voltage is a measure of the amount of recombination in the solar cell [12, 13]. Short circuit current and open circuit voltage are the maximum current and voltage of the solar cell, respectively. However, the power obtained from the solar cell is zero at both operating points. The point on the J–V curve that produces the maximum power is indicated as the maximum power point, where the current density represents the maximum current J_{max} and the applied voltages represent the maximum voltage V_{max}.

3- Fill factor FF: is the measurement of quality or performance of the solar cell. It determines the maximum power of the solar cell and is defined as the ratio between the maximum powers generated from the solar cell $P_{max} = J_{max} \times V_{max}$ to the theoretical value of the power i.e. the product of the short circuit current to the open circuit voltage, which is given by the following relationship:

$$FF = \frac{V_{max} J_{max}}{V_{oc} J_{sc}} \quad \ldots\ldots\ldots\ldots (5)$$

4- Conversion Efficiencyη: this factor depends on the type and intensity of the solar spectrum as well as the temperature of the solar cell. It is defined as the ratio between the maximum powers coming out of the solar cell P_{max} to the input power P_{in}, as given by the following equation [14]:

$$\eta = \frac{V_{max} J_{max}}{P_{in}} = \frac{V_{oc} J_{sc} FF}{P_{in}} \quad \ldots\ldots\ldots\ldots (6)$$

Current - Voltage Characteristics of the Solar Cell

The current-voltage properties of the photovoltaic device can represent graphically the operation of the solar cell and consist of the matching of the current-voltage properties of the solar cell in dark (in the absence of light) with the current generated under lighting state. As the solar cell in the dark state possesses the same properties of the dual device, then when light falls on it, the electrical power can

be extracted from the bottom of the current-voltage properties curve, in the fourth quarter, where the voltage is positive and the current is negative. Thus, the lighting current is added to the dark current in the solar cell, where the current density of the total photodiode is given as follows [15]:

$$J = J_{sc} - J_{dark} \quad \ldots\ldots\ldots\ldots (7)$$

where J_{sc} and J_{dark} represent the short-circuit current and the dark current, respectively, as given by the following equation:

$$J_{dark} = J_o \left(e^{qV/nkT} - 1\right) \quad \ldots\ldots\ldots\ldots (8)$$

By substituting the value of the dark current, the total current density of the diode represents the following:

$$J = J_{sc} - J_o \left(e^{qV/nkT} - 1\right) \quad \ldots\ldots\ldots\ldots (9)$$

where J_o is the saturation current density in the dark state [16].

Materials and methods

The experimental arrangement of the exposed (Si) p-n junction apparatus is illustrated in Fig. 1.

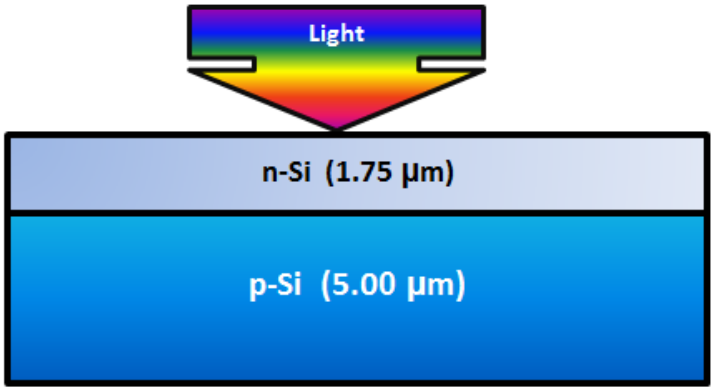

Figure 1- Diagram of the experimental arrangement of dual device (Si) p-n junction.

Different spectra of light were used for solar radiation falling to the Earth surface. Using the data for the SCAPS-1D simulation program, those spectra were drawn as shown in Fig. 2, as follows:

1- The normal solar radiation (AM 1.5) standard spectrum is shown in Fig. 2. Its wavelengths range 250 - 2500 nm, whereas the maximum intensity of solar radiation at wavelength 500 nm has a maximum of 2.00E-5 W/m^2/nm. The figure indicates two spectra of solar radiation, which are the vertical direct solar radiation and the total solar radiation falling on the hemispherical Earth surface 2π on inclined solar panels at an angle of 38^o [7].

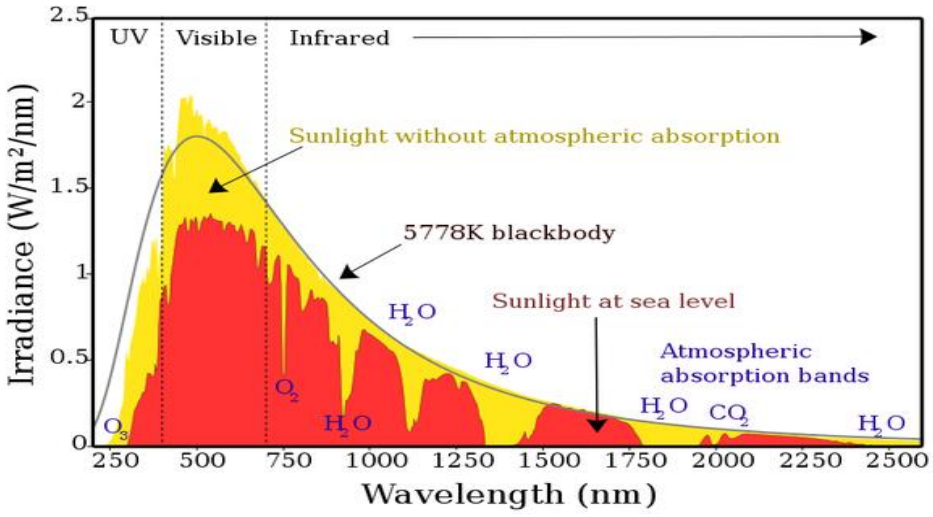

Figure 2- Diagram of solar radiation (AM 1.5) Standard Spectrum falling to the Earth's surface.

2- Black body spectrum, which is shown in Fig. 3-a, is similar to the limit of the normal solar spectrum. Its parameters indicate wavelengths range of 300-4000 nm and a maximum intensity, at wavelength 500 nm, of up to 1.43E-04 W/cm^2/nm.

3- White spectrum constant photon flux: as shown in Fig. 3-b, this region included all the solar spectra, indicating wavelengths range of 400-800 nm, while the maximum intensity of solar radiation at wavelength 400 nm is up to 7.75 E-05 W/cm^2/nm. However, the area of illumination intensity was greater than the area of black-body radiation spectrum, and the total sum of incident photons was 6.242E-16 photons/cm^2/s.

4- White spectrum constant photon power: as shown in Fig. 3-c, this region included all solar spectra between 400-800 nm. The maximum intensity of solar radiation at this region was 2.50E-04W/cm^2/nm and the area of the intensity of illumination was greater than the area of the spectrum of white light fixed photon flood.

5- Monochromatic spectrum constant flux: as shown in Fig. 3-d, this region included all the solar spectra between 594.8-605.1 nm, while the maximum intensity of solar radiation was about 2.07E-03 W/cm^2/nm, which had a higher illumination than previous spectra.

6- Monochromatic spectrum constant power spectrum: as shown in Fig. 3-e, this region included all the solar spectra between 594.8-605.1 nm, while the maximum intensity of solar radiation was about 1.00E-02 W/cm^2/nm, which was the highest illumination intensity of the fixed-wave monochromatic spectrum.

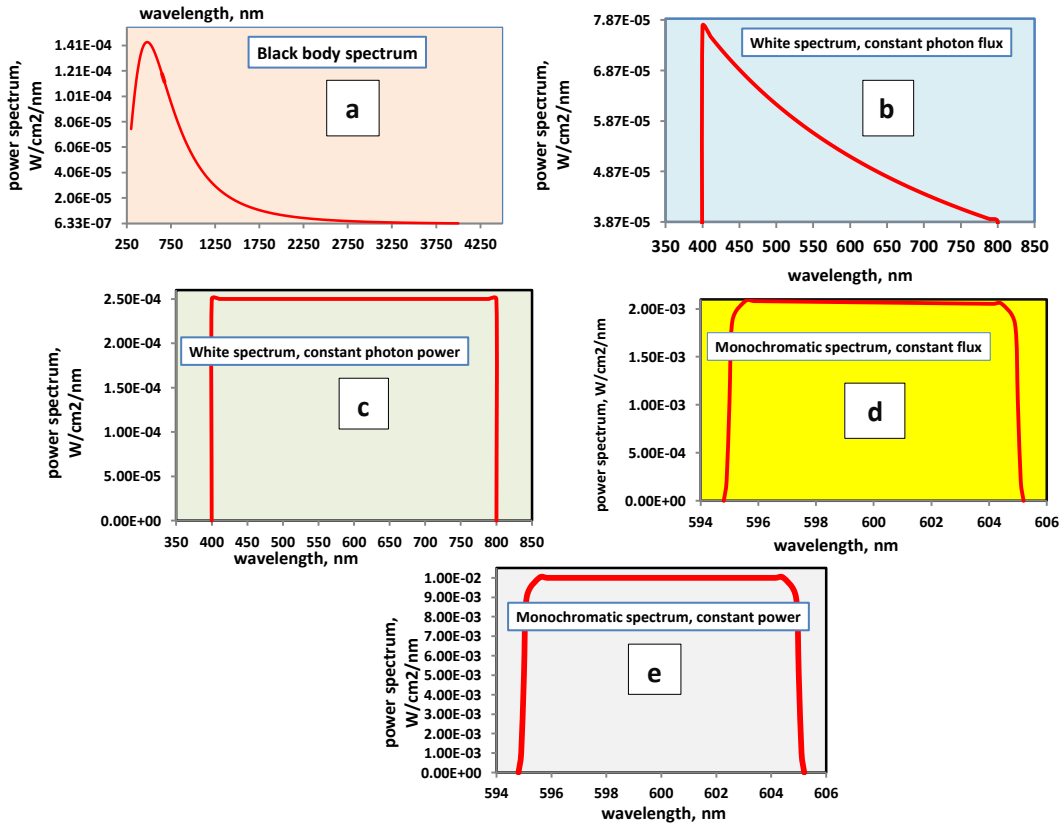

Figure 3- The spectra of solar radiation**. (a)** Black body spectrum. **(b)** White spectrum constant photon flux. **(c)** White spectrum constant photon power. **(d)** Monochromatic spectrum constant flux. **(e)** Monochromatic spectrum constant power spectrum

Results and discussion

1- Thickness test

After entering the special parameters for both the p-Si and n-Si layers of the dual device diode, shown in Fig. 4. The SCAPS-1D computer program was applied to simulate the thickness of the p-Si and n-Si layers to obtain the ideal thickness of the pn-Si dual device using the bath set-up package gate, as shown in Figure (5).

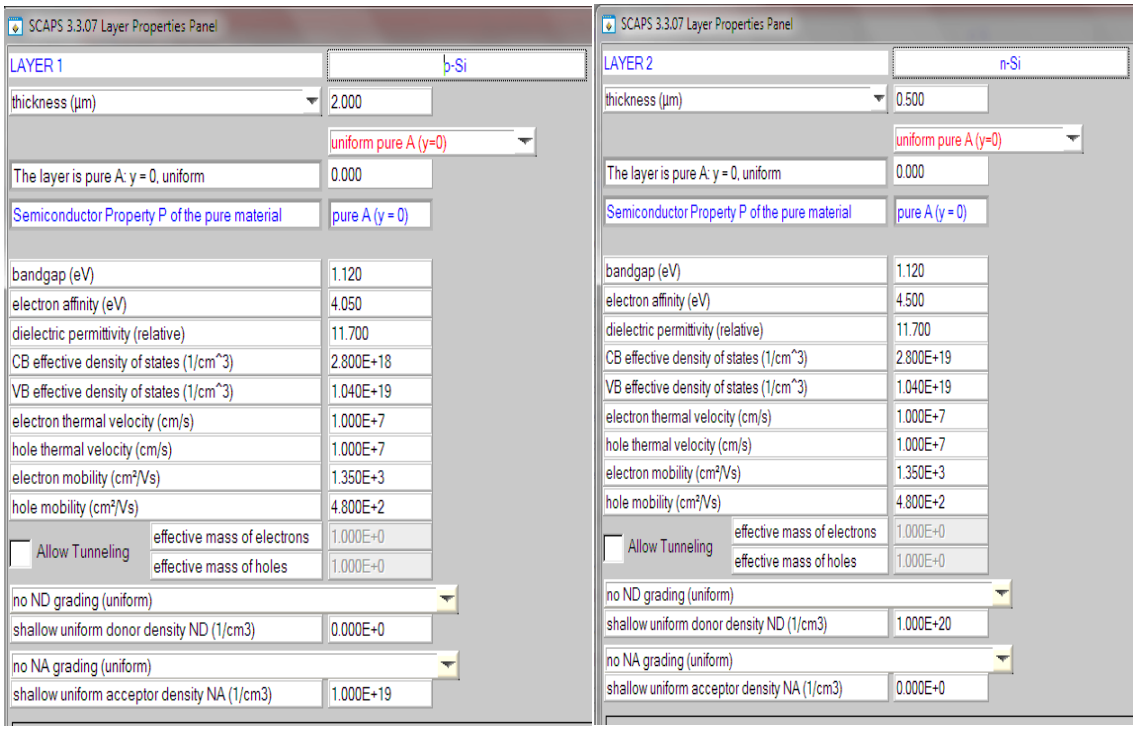

Figure 4-Specific parameters for the p-Si and n-Si layers

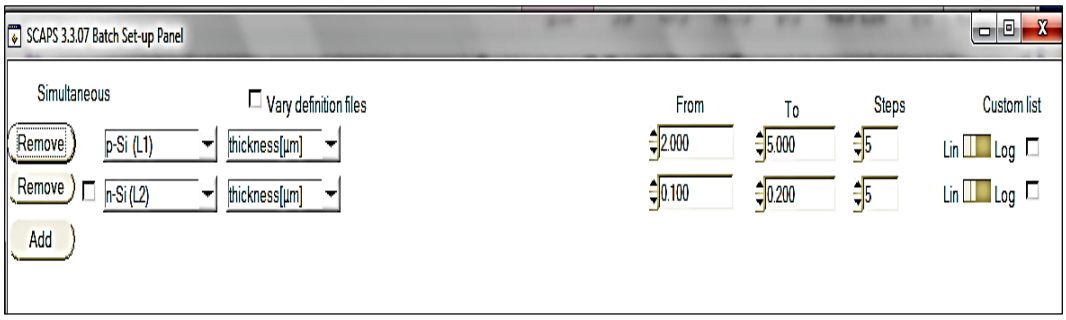

Figure 5-Specific parameters for thicknesses of the p-Si and n-Si layers for the beam gate.

The thickness of each of the two layers was tested after choosing thickness of the p-Si layer between of 1-5 µm, while the thickness of the n-Si layer was between 0.1-0.2 µm. The results obtained are shown in Fig. 6, which shows the relationship of the layer change p-Si (2-5)µm, after fixing the thickness of X layer to (n-Si) = 1.75µm, with {V_{OC} ،$J_{SC,}$ FF%, η%, V_{MPP} ،J_{MPP}}.

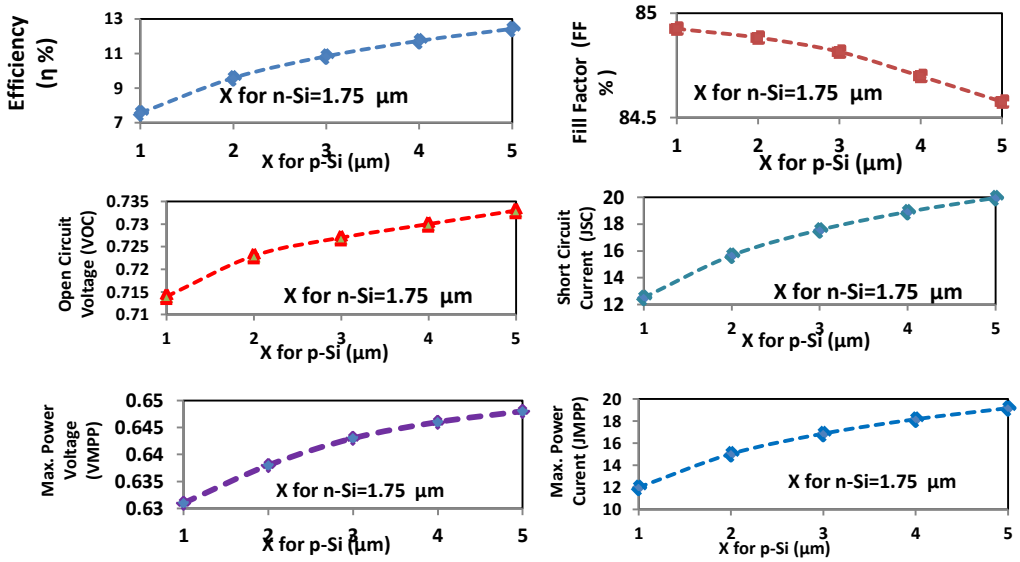

Figure 6- Thickness of the p-Si and n-Si layers with {V_{OC} ،$J_{SC,}$ FF%, η%, V_{MPP} ،J_{MPP}}.

At a thickness of X (p-Si) = 5µm and when X (n-Si) = 1.75µm, by using normal solar spectrum at temperature 300K, so the final results getting are {V_{OC} = 0.73V, J_{SC} = 19.96mA/cm^2, FF = 84.93%, eta(η) =12.42%, V_{MPP} = 0.6482V and J_{MPP} = 19.1598mA/cm^2}.This results agrees with the recent application requirements for solar cells [1], whose efficiency must be higher than eta(η) =12.42%, after testing the optimum thickness of the dual p-Si devices. When compared with other thicknesses usered.

After fixing both layers X (p-Si) = 5µm and X (n-Si) = 1.75µm, we show the results in Fig. 7.

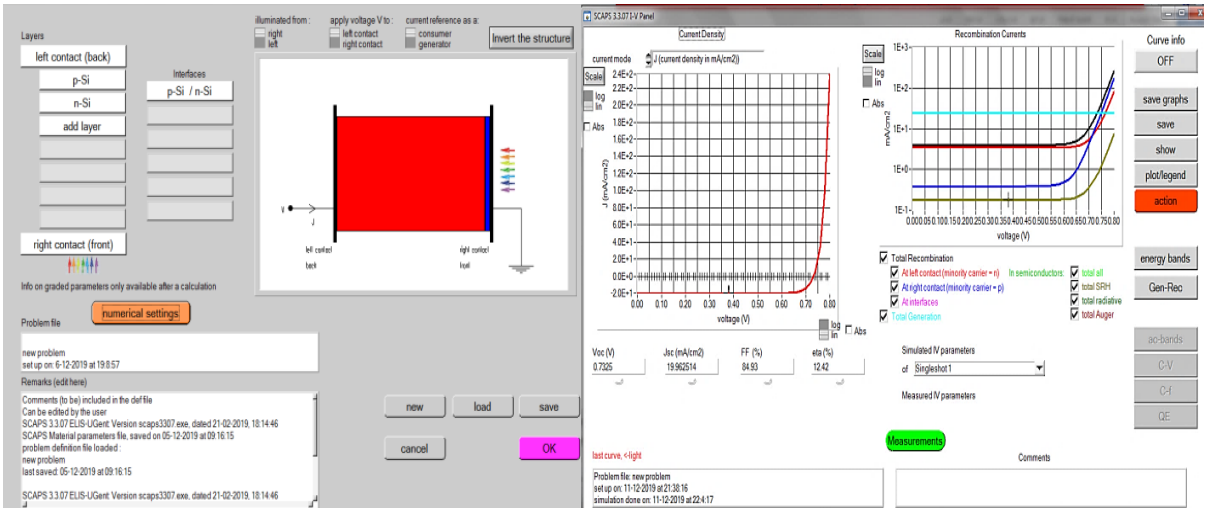

Figure 7- Results obtained from applying thickness for both p-Si and n-Si layers from the beam gate.

2- Testing the working solar spectrum

Solar spectrum models were applied using the SCAPS-1D computer program to simulate the effects of the solar spectrum on both p-Si and n-Si layers, when projected temperature was fixed at

300K, to obtain the output values. Hence, the properties of the special (I-V) characteristics are {V_{OC} ، $J_{SC,}$ FF%, η%, $V_{MPP,}$ J_{MPP}}.

Table 1- Results obtained from the application of the work of the solar spectrum for both p-Si and n-Si layers at 300K

	Spectrum Model	V_{OC} (Volt)	J_{SC} (mA/cm^2)	FF %	η %	V_{MPP} (Volt)	J_{MPP} (mA/cm^2)
1	Black body spectrum	0.7324	19.8232	84.896	12.30	0.6480	19.0205
2	AM1_5G 1 sun. spectrum	0.7326	19.9625	84.925	12.42	0.6482	19.1598
3	White spectrum, constant photon flux	0.7052	6.91111	84.540	19.17	0.6220	6.6246
4	White spectrum, constant photon power	0.7444	31.3839	85.061	19.86	0.6593	30.1406
5	Monochromatic spectrum, constant flux	0.7064	7.2604	84.606	21.07	0.6232	6.9629
6	Monochromatic spectrum, constant power	0.7472	35.1374	85.146	22.43	0.6621	33.7629

3- Testing the effects of temperature on the device

Solar spectrum models, as shown in Table 1, and using the SCAPS-1D computer program, were applied in simulating the effects of temperature values of 250K, 300K, 350K and 400K in p-Si and n-Si. The models were adopted to obtain output values of the special characteristics of the voltage-current (I-V Characteristics), which are V_{OC} ،$J_{SC,}$ FF%, Efficiency eta (η%), V_{MPP} ، and J_{MPP}, where V_{MPP} and J_{MPP} represent maximum power voltage and maximum power current, respectively, as shown in Fig's.(8, 9, 10, 11, 12, 13).

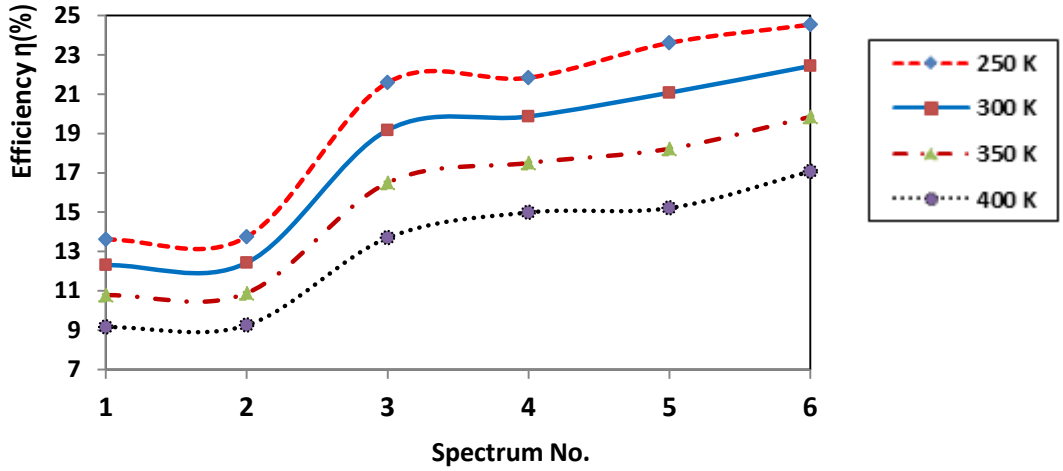

Figure 8- Results obtained from applying the effect of temperature to the p-Si and n-Si layers to obtain the Efficiency eta (η%) of the device and at different solar spectrum as shown in Table 1.

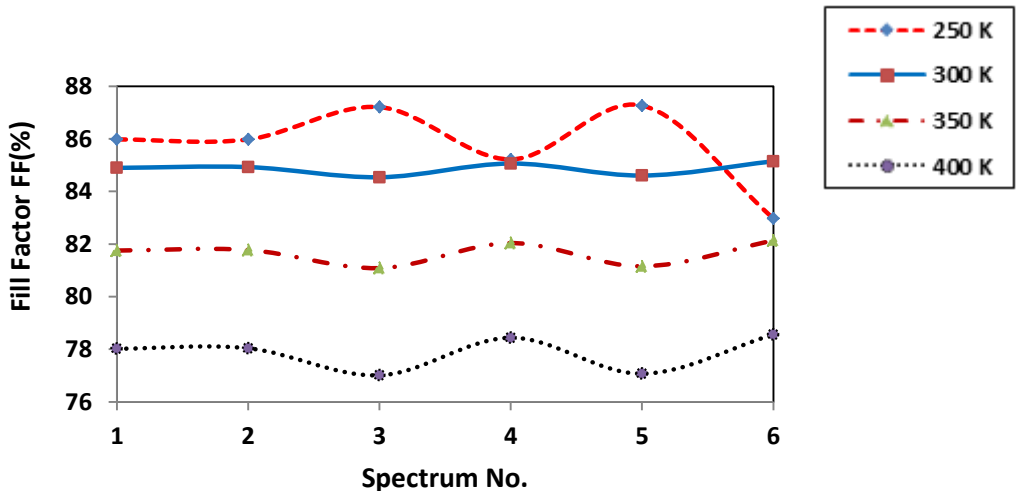

Figure 9-Results obtained from applying the effect of temperature on p-Si and n-Si layers to obtain the filling factor (FF%) of the device at different solar spectra shown in Table 1.

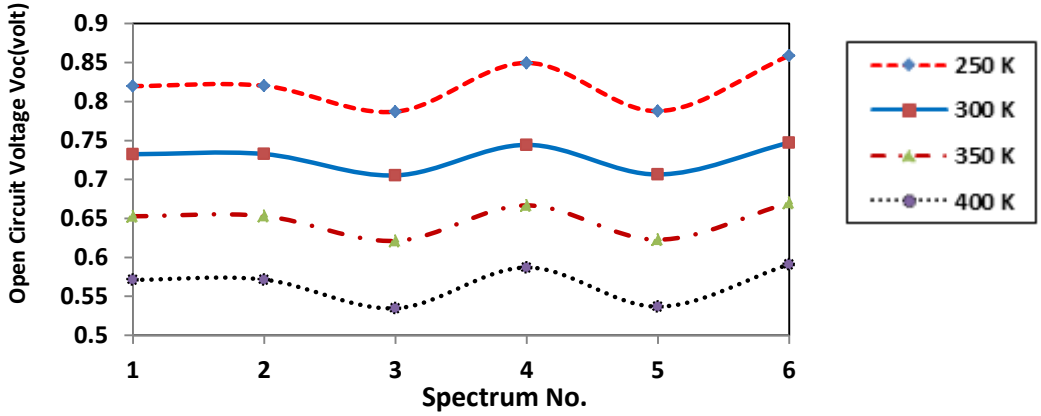

Figure 10- Results obtained from applying the effect of temperature on p-Si and n-Si layers to obtain the open circuit voltage (V_{OC}) of the device at different solar spectra shown in table 1.

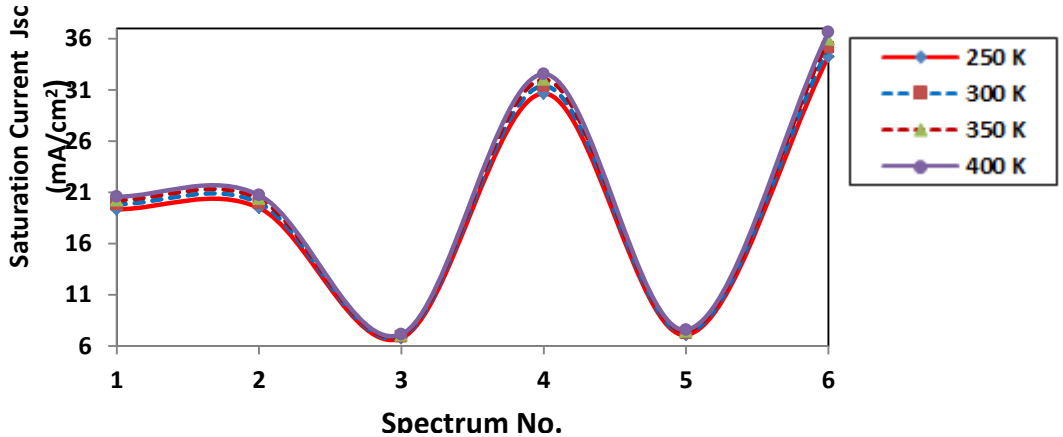

Figure 11- Results obtained from applying the effect of temperature for p-Si and n-Si layers to obtain the saturation reverse current (J_{SC}) of the device and at different solar spectrum as shown in Table 1.

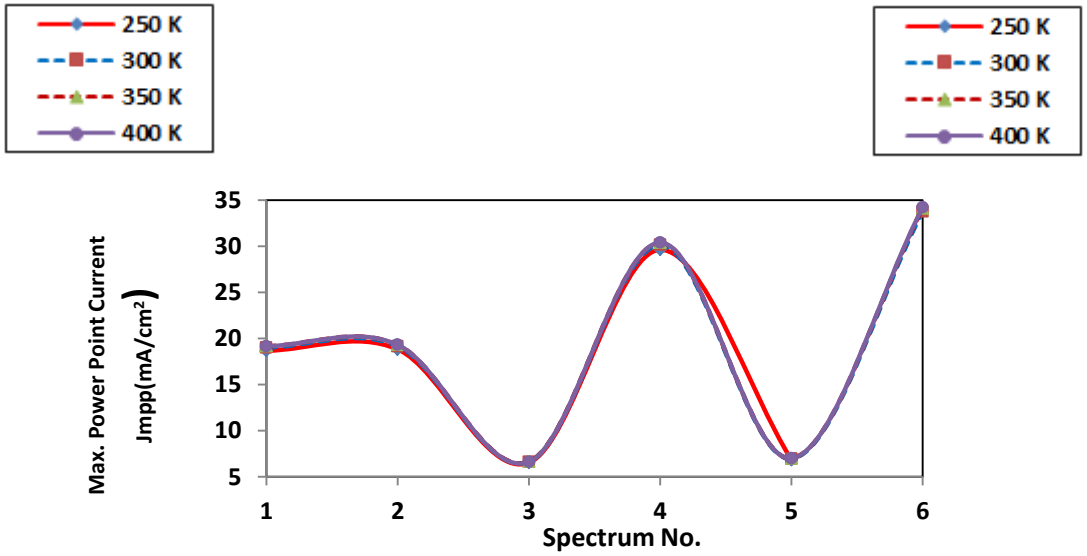

Figure 12-Results obtained from applying the effect of temperature on p-Si and n-Si layers to obtain the maximum power voltage (J_{MPP}) of the device at different solar spectra shown in Table 1.

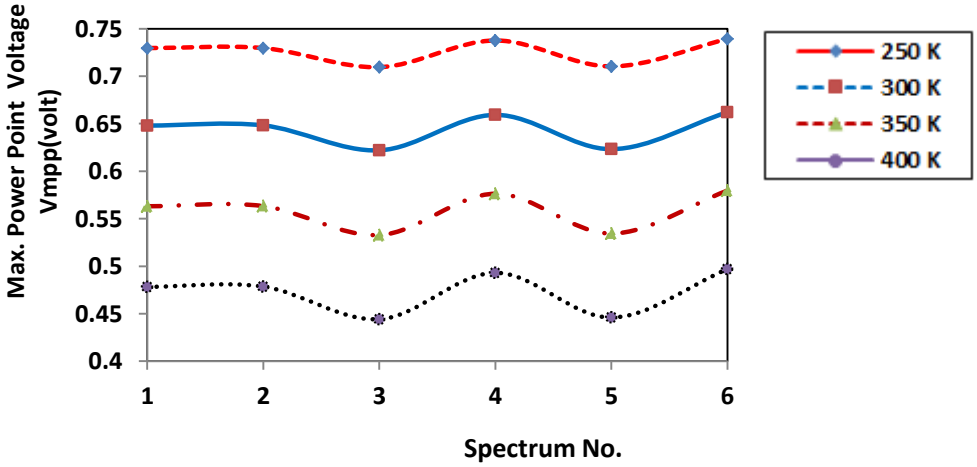

Figure 13- Results obtained from applying the effect of temperature on p-Si and n-Si layers to obtain the maximum current power (V_{MPP}) of the device at different solar spectra shown in Table 1.

The effects of different solar spectra were studied, which are, respectively, the Black body spectrum, White spectrum, constant photon flux, White spectrum, constant photon power, Monochromatic spectrum, constant flux, Monochromatic spectrum constant flux, and Monochromatic spectrum constant power spectrum). The highest values obtained in all properties of the current-voltage IV were at the Monochrome spectrum constant power (V_{OC}=0.74 V, J_{SC}=35.1 mA/cm^2, FF = 85.1 %, eta (η)% = 22.4, V_{MPP}=0.66 V, and JMPP = 33.76 mA/cm^2), which agrees with the results of an earlier work [14].

4- Effects of both Front and Back bias on the device

Solar spectrum models were applied using the SCAPS-1D computer program to simulate the effects of both right contact (Front) and left contact (Back) on both p-Si and n-Si layers. The aim was to obtain the output values of the IV Characteristics, which are V_{OC} ،$J_{SC,}$ FF%, η%, V_{MPP} ، and J_{MPP} as in Fig's.(14, 15, 16, 17, 18, 19).

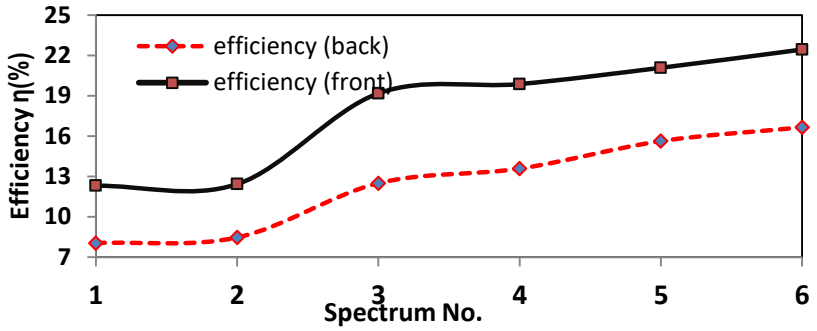

Figure 14-Results obtained from applying different solar spectra, shown in Table 1), on p-Si and n-Si layers to obtain the efficiency eta (η%) of the device at the Forward and backward bias**.**

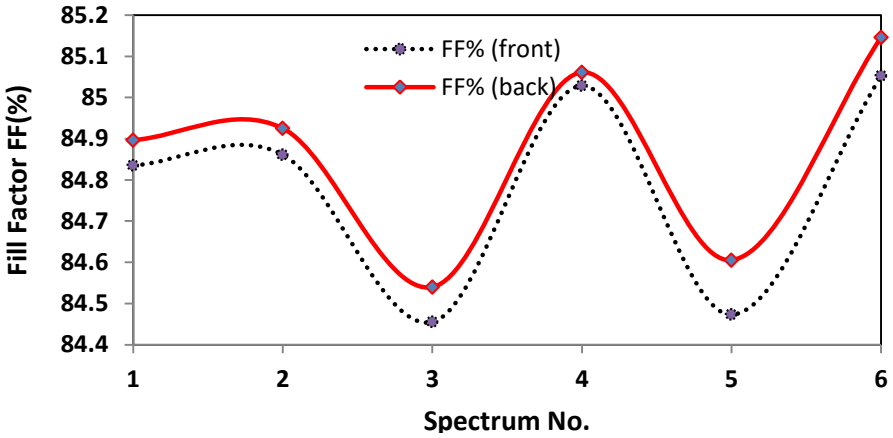

Figure 15- Results obtained from applying different solar spectra, shown in Table 1, on p-Si and n-Si layers to obtain the Fill Factor (FF%) of the device at the forward and backward bias**.**

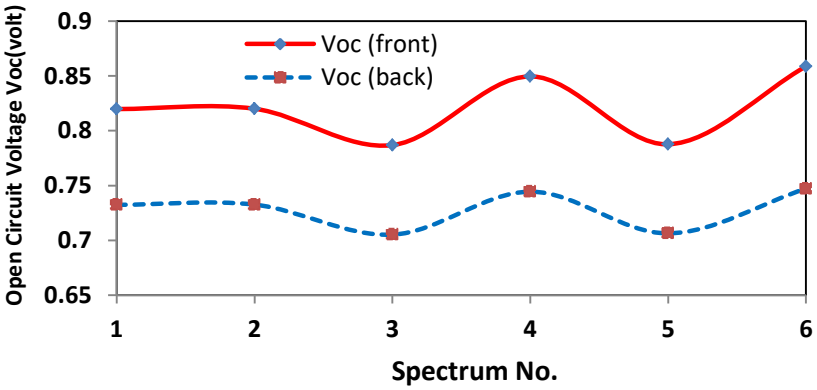

Figure 16-The final results obtained from applying the effect of the different solar spectrum shown in Table 1, on p-Si and n-Si layers to obtain the open circuit voltage (V_{oc}) of the device at the forward and backward bias**.**

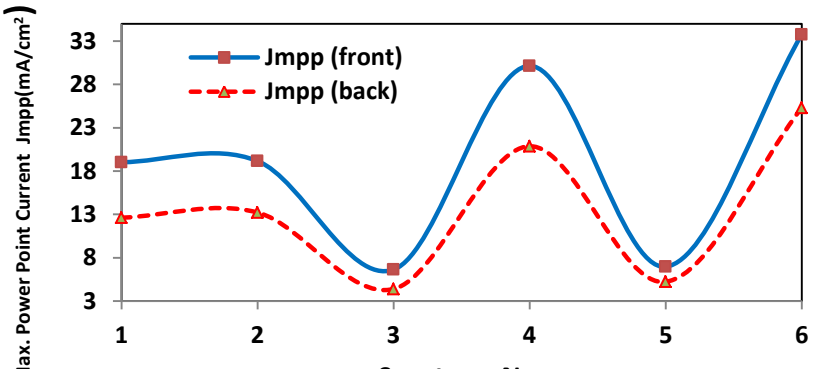

Figure 18- The final results obtained from applying different solar spectra, shown in Table 1, on p-Si and n-Si layers for Maximum Potential Voltage (V_{MPP}) for the device at the forward and backward bias**.**

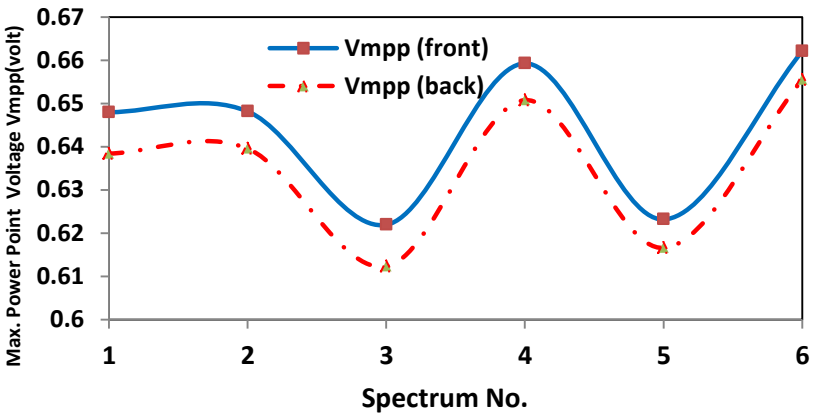

Figure 19- The final results obtained from applying different solar spectra, shown in Table 1, on p-Si and n-Si layers for maximum current power capacity (J_{MPP}) the for the front and back bias.

Conclusions

In this study, a simulation was performed on a pn-Si device using one dimension computer program SCAPS-1D. It was found that the best efficiency of the device is obtained eta (η) = 12.4% by using the normal solar spectrum M1_5G 1 at 300 K, when the optimum thickness of the p-layer is 5 µm and that for the n-layer is 1.75 µm.

It was also found from studying the effects of different solar spectra that the highest values of all I-V characteristics were obtained at the monochromatic spectrum of constant power, where the optimum efficiency of the pn-Si was eta (η) = 22.4 %.

When we studied the effects of different temperatures on the six solar spectra models, and after performing a simulation on the device, it was found that the highest values for both efficiency and fill factor were eta (η)=24.54% and FF=87.26%, respectively, at a monochromatic spectrum of constant power, when the temperature was 250K.

Also, we found that the forward bias gave the best results obtained from the monochromatic spectrum of constant power as compared to those from the reverse bias in all of the IV characteristics , where (η) = 22 % at the forward bias and (η) =16 % at the reverse bias.

References

1. S. M. Sze, Semiconductor Devices Physics and Technology, 3rd ed. John Wiley and Sons, Singapore, (1985).
2. M. J. Madou, Fundamentals of Micro Fabrication and Nanotechnology ,CRC Press, Taylor & Francis Group, Boca Raton FL, Vol. II. 9J, (2012).
3. Nelson, The Physics of Solar Cells ,Imperial College Press, UK, (2003).
4. Ryan P. Smith, Angela An-Chi Hwang, Tobias Beetz, and Erik Helgren, Introduction to semiconductor processing: Fabrication and characterization of p-n junction silicon solar cells, Am. J. Phys. 86 (10), (2018).
5. Peter Würfel and Uli Würfel, Physics of Solar Cells From Basic Principles to Advanced Concepts, 3rd ed. 2016 Wiley-VCH Verlag GmbH & Co.
6. **6-** M. Burgelman, J. Verschraegen, S. Degrave, P. Nollet, Prog. Photovoltaics 12 (2–3) (2004).
7. M. Burgelman, J. Verschraegen, S. Degrave and P.Nollet, Modeling Thin-film PV Devices, Prog. Photovolt: Res. Appl. (2003).
8. R.B. Bird, W.E. Stewart, and E.N. Lightfoot, "Transport Phenomena," Wiley, (2007).

A. Akinpelu, M. Usikalu, C.A. Onumejor, and T. Arijaje, A Numerical Simulation and Modeling of Poisson Equation for Solar Cell in 2 Dimensions, Conference Paper *in* IOP Conference Series Earth and Environmental Science· July (2018).

9. M. Burgelman , P. Nollet, S. Degrave, Modeling polycrystalline semiconductor solar cells, Thin Solid Films, 527-532 (2000).
10. Usha Mandadapu, S. Victor Vedanayakam1 and K. Thyagarajan, Simulation and Analysis of Lead based Perovskite Solar Cell using SCAPS-1D, Indian Journal of Science and Technology, Vol 10(11), February (2018).
11. Faisal Baig, PH.D Thesis, Numerical Analysis for Efficiency Enhancement of Thin Film Solar Cells, Universitat Politècnica de València, (2019).
12. Hongmei Dang, "Nanostructured Semiconductor Device Design in Solar Cells", Ph.D. Thesis, University of Kentucky (2015).
13. Amu, Tochukwu Loreta, MSc. Thesis, Performance Optimization of Tin Halide Perovskite Solar Cells via Numerical Simulation, African University of Science and Technology, Abuja, Nigeria (2014).
14. Tariq A. Mohammed , Ayed N. Saleh, Study the effect of thickness and reflectivity on (n-ZnSe / p-MASnI3 / p-CuSCN) solar cell properties using SCAPS-1D, Tikrit Journal of Pure Science Vol. 24(7) (2019).
15. E.M.G. Rodrigues, R. Melício, V.M.F. Mendes and J.P.S. Catalão, Simulation of a Solar Cell considering Single-Diode Equivalent Circuit Model, RE&PQJ, Vol.1, No.9, May (2011).